



ORIGINAL ARTICLE

Open Access



Leveraging quorum sensing system for automatic coordination of *Escherichia coli* growth and lactic acid biosynthesis

Chang Ge, Shunqi Run, Hongkai Jia and Pingfang Tian*

Abstract

Purpose: Overproduction of desired metabolites usually sacrifices cell growth. Here we report that quorum sensing (QS) can be exploited to coordinate cell growth and lactic acid production in *Escherichia coli*.

Methods: We engineered two QS strains: one strain overexpressing acyl-homoserine lactone (AHL) synthesis genes ("ON"), the other strain overexpressing both AHL synthesis and degradation gene (*aiiA*) ("ON to semi-OFF"). To clarify the impact of the QS system on lactic acid production, D-lactate dehydrogenase gene *ldhA* was deleted from the *E. coli* genome, and Enhanced Green Fluorescence Protein (eGFP) was used as the reporter.

Results: Compared to the "ON" strain, the "ON to semi-OFF" strain showed delayed log growth and decreased *egfp* expression at stationary phase. When *egfp* was replaced by *ldhA* for lactic acid production, compared to the wild-type strain, the "ON to semi-OFF" strain demonstrated 231.9% and 117.3% increase in D-lactic acid titer and space-time yield, respectively, while the "ON" strain demonstrated 83.6%, 31%, and 36% increase in growth rate, maximum OD₆₀₀, and glucose consumption rate, respectively. Quantitative real-time PCR revealed that both *ldhA* and the genes for phosphotransferase system were up-regulated in *ldhA*-overexpressing "ON" strain compared to the strain only harboring QS system. Moreover, the "ON" strain showed considerable increase in glucose consumption after a short lag phase. Compared to the reference strain harboring only *ldhA* gene in vector, both the "ON" and "ON to semi-OFF" strains demonstrated synchronization between cell growth and D-lactic acid production.

Conclusions: Collectively, QS can be leveraged to coordinate microbial growth and product formation.

Keywords: *E. coli*, Quorum sensing, Lactic acid, Cell growth, Automatic regulation

Background

One primary mission of microbial metabolic engineering and synthetic biology is the high-level production of intended metabolites. To this end, scientists have developed a set of strategies, including overexpression of key enzymes, deletion or attenuation of competing pathways (Jiang et al. 2021; Wu et al., 2020a, b; Mazumdar et al. 2010), management of ATP (Lan and Liao 2012),

and adjustment of cofactors (Ling et al. 2018). However, these strategies, in most cases, compromise cell growth and hamper product formation (Liu et al. 2019). To coordinate cell growth and production formation, both static and dynamic control approaches have been developed. Static control strategies include in situ recovery of desired metabolites (Kaur et al. 2015), optimization of fermentation conditions, improvement of cell tolerance (Lou et al. 2018), enzyme immobilization, and enzyme modification to circumvent feedback inhibition (Chen et al. 2014). Unlike static control approaches that ignore the changing environments, dynamic approaches enable real-time sensing of changing settings (Zhou et al. 2012;

*Correspondence: tianpf@mail.buct.edu.cn
Beijing Key Laboratory of Bioprocess, College of Life Science and Technology, Beijing University of Chemical Technology, Beijing 100029, People's Republic of China



© The Author(s) 2022. **Open Access** This article is licensed under a Creative Commons Attribution 4.0 International License, which permits use, sharing, adaptation, distribution and reproduction in any medium or format, as long as you give appropriate credit to the original author(s) and the source, provide a link to the Creative Commons licence, and indicate if changes were made. The images or other third party material in this article are included in the article's Creative Commons licence, unless indicated otherwise in a credit line to the material. If material is not included in the article's Creative Commons licence and your intended use is not permitted by statutory regulation or exceeds the permitted use, you will need to obtain permission directly from the copyright holder. To view a copy of this licence, visit <http://creativecommons.org/licenses/by/4.0/>.

Tan and Prather 2017; Harder et al. 2018). For instance, metabolite-sensitive biosensors can timely mitigate metabolic stress (Xu et al. 2014; Peters et al. 2018).

Apart from the aforementioned strategies, microbes have evolved exquisite mechanisms to coordinate cell growth and metabolite accumulation. For instance, quorum sensing (QS) represents a cell-to-cell communication tailored for governing cell density and other biochemical events (You et al. 2004; Moreno-Gómez et al., 2017). The LuxI/R QS system from *Vibrio fischeri* relies on an extracellular signal molecule termed autoinducers such as N-acyl homoserine lactone (AHL) (Papenfort and Bassler 2016). AHL is a typical autoinducer identified in bacteria-harboring enzymes LuxI (N-acyl homoserine lactone synthase) and LuxR (AHL-binding transcription inducer). The LuxI catalyzes the formation of AHL, while *luxR* encodes an AHL-binding transcription factor (Fuqua et al. 1994). Interestingly, the enzyme, AiiA (N-acyl homoserine lactone hydrolase), from *Bacillus thuringiensis* can degrade AHL and thereby quench QS (Dong et al. 2000; Dong et al. 2001; Dong et al. 2002; Thomas et al. 2005). AHL can pass through the cell membrane, and when AHL concentration reaches a threshold, cells start to orchestrate a series of biochemical events including bioluminescence, biofilm formation, and signal transduction. It is costly for a single cell to accomplish all the aforementioned events. However, the QS mechanism is cost-effective, as it is a collective behavior. The LuxI/R QS represents a naturally occurring strategy to balance cell growth and other events, and holds promise to switch gene expression. Apart from LuxI-type QS system, other QS systems can also coordinate cell growth and other events (Balestrino et al. 2005; Sun et al. 2016).

High-level product formation, in most cases, imposes a heavy burden on cell growth. For instance, buildup of lactic acid impairs cell growth and therefore restricts its overproduction (Zhou et al., 2006a, b). As an important metabolism, the biosynthesis of D-lactic acid is mainly accomplished by D-lactic acid dehydrogenase (LdhA) (Bunch et al. 1997), a reversible enzyme in *Escherichia coli*. While low concentration of lactic acid is beneficial for cell growth, a high concentration of lactic acid inhibits cell growth (Zhou et al., 2006a, b). Given the close relation between QS and cell growth, the factors influencing cell growth should also affect QS activity. That is, the QS system functionally responds to metabolite stress. To date, QS has been exploited for metabolic engineering and synthetic biology purposes. For example, QS was exploited for an automatic switch of metabolic states (Kim et al. 2017). Also, QS is capable of spatial regulation of gene expression when coupled with RNA interference (RNAi) (Williams et al. 2015) or CRISPR-dCas9 (Gupta et al. 2017; Doong et al. 2018).

More importantly, QS has been harnessed for automatic drug delivery (Din et al. 2016).

Given the above information, we conjecture that reengineering of the innate QS circuit holds promise to balance cell growth and lactic acid formation. To test this hypothesis, lactic acid synthesis gene *ldhA* was knocked out from the *E. coli* genome, leading to a chassis cell. Next, two QS-based strains were engineered. One strain harboring AHL synthesis genes was named "ON". The other strain harboring both AHL synthesis and degradation genes was designated "ON to semi-OFF". Enhanced green fluorescent protein (eGFP) was used as the reporter to characterize the engineered QS systems. Coexpression of *ldhA* and QS cassette was to dissect the influences of two QS systems on lactic acid production. Detailed analysis of protein expression, cell growth, glucose consumption, D-lactic acid, and byproducts was to decipher the impacts of QS circuits on microbial metabolisms. Quantitative real-time PCR (qRT-PCR) analysis of the genes related to QS and glucose metabolisms was to clarify the underlying mechanisms. Overall, this study aims to develop a QS-based dynamic control approach for coordinating cell growth and lactic acid production.

Materials and methods

Strain, vector, medium, and reagents

Strains and vectors used in this study are listed in Table S1. *E. coli* BL21(DE3) was purchased from Biomed Co. Ltd. Strains were stored in glycerol-containing Luria-Bertani medium at -20°C . Prior to culture, they were incubated to test tubes containing 4 mL Luria-Bertani medium and appropriate antibiotics, and shaken at $180 \times g$ and 37°C . For seed culture, *E. coli* was incubated in M9 minimal medium containing the following components per liter: glucose, 3.1 g; NaCl, 0.5 g; $\text{Na}_2\text{HPO}_4 \cdot 7\text{H}_2\text{O}$, 12.8 g; KH_2PO_4 , 3.0 g; NH_4Cl , 1.0 g; MgSO_4 , 0.492 g; $\text{CaCl}_2 \cdot 6\text{H}_2\text{O}$, 0.0219 g. One percent (v/v) of seed culture was transferred to a 250-mL flask containing 100 mL M9 minimal broth and appropriate antibiotics, and cultured in a shaker at $150 \times g$ and 30°C . The concentrations of kanamycin and chloramphenicol were 50 $\mu\text{g}/\text{mL}$ and 34 $\mu\text{g}/\text{mL}$, respectively. Vectors pKD46, pKD13, and pCP20 were used for gene knockout (Datsenko and Wanner, 2000). Other vectors used in this study were derived from vector pACYC-Duet1 or pET-28a. Restriction endonucleases and DNA polymerase were purchased from TaKaRa (Dalian, China). Kits for ligation were purchased from Thermo (Beijing, China). Kits for plasmid isolation and DNA purification were purchased from Biomed (Beijing, China). DNA marker and other reagents were purchased from Bioroyee (Beijing, China). Gene synthesis and DNA sequencing were accomplished by BGI (Beijing, China) and Beijing Syngentech Co., Ltd. Standards

for metabolite assay were products of Sigma (Beijing, China).

Gene knockout

The *E. coli ldhA* gene was knocked out using the reported method (Datsenko and Wanner, 2000). To obtain cassette 52nt-FRT-Kan-FRT-50nt, PCR primers were designed according to the 52-nt upstream and 50-nt downstream sequence immediately flanking the *ldhA* gene (Table S2). The kanamycin resistance gene (KanR) and two FRT (FLP recognition target) sites were cloned by PCR from vector pKD13. The 50- μ L mixture for PCR reaction included 25 μ L of Premix PrimeSTAR[®] HS, 1 ng of pKD13, 0.4 mM of forward, and reverse primers of pKD13. The protocol for PCR reaction includes initial denaturation at 98°C for 2 min, followed by 30 cycles of 98 °C for 10 s, 60 °C for 50 s, 72 °C for 110 s, and 72°C for 10 min. The Dpn I endonuclease was used to digest vector pKD13.

The competent *E. coli* BL21 cells were electro-transformed with vector pKD46 and incubated in Luria-Bertani medium at 30 °C for 1 h. Positive recombinants were screened by Luria-Bertani ampicillin plates. After overnight cultivation, positive recombinants were confirmed by colony PCR. The strains harboring vector pKD46 were grown in Luria-Bertani medium to reach OD₆₀₀ of 0.12–0.2. Next, 100 mM L-arabinose was used to induce recombinase expression at 37°C for 1.5 h. The strains were concentrated by 30-fold at 4 °C and washed twice with cold distilled water. Electroporation was performed in Bio-rad Micropulser with 100 μ L competent cells and 5 μ L PCR products added in a 0.2-cm cuvette. The transformed cells were recovered in 890 μ L Luria-Bertani medium at 30°C for 2 h, and then grown in kanamycin Luria-Bertani plate at 30 °C for 72 h. Positive clones were confirmed by colony PCR and DNA sequencing.

Vector pCP20 harbors ampicillin and chloramphenicol resistance genes (Amp^R and Cm^R), temperature-sensitive replication, and FLP sequence for acting on two FRT sites. After pCP20 was transformed into competent *E. coli* cells, the kanamycin resistance gene on *E. coli* chromosome was eliminated upon cultivation at 30°C for 24 h. The resulting Kan^R mutant was continuously grown in an antibiotics-free Luria-Bertani plate at 42°C for 3–5 generations of subculture, and then grew in Luria-Bertani plate containing ampicillin and chloramphenicol to examine whether the strains still harbored vector pCP20. Mutant *E. coli* Δ *ldhA* was confirmed by colony PCR and DNA sequencing.

Construction of recombinants

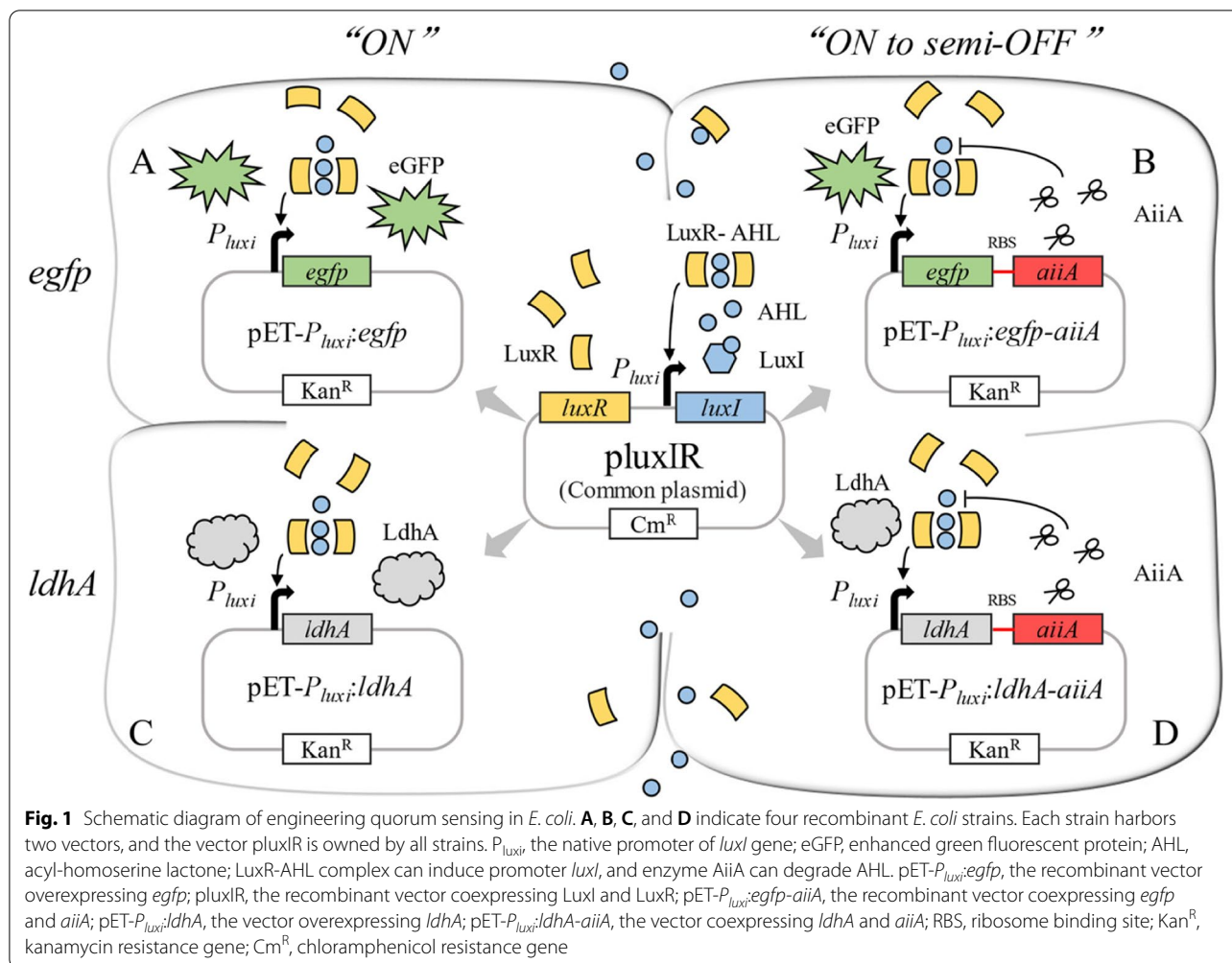
The AHL synthesis gene cluster *luxI-luxR* from *V. fischeri* ES114 (Papenfort and Bassler 2016) was cloned by PCR and inserted into vector pACYCDuet1 at *Bam*H I/*Eco*R

I, leading to vector pluxIR which served as the common vector for all recombinant strains (Fig.1). To construct an AHL-responsive vector, the original T7 promoter in vector pET-28a(+) was replaced by an AHL-inducible *luxI* promoter, resulting in vector pET-*P_{luxI}*. To determine the influence of AHL on lactic acid production, a set of vectors were constructed. The genes—*egfp* (followed by *ssrA* degradation tag: GCTGCTAACGACGAAAACACTAC GCTCTGGCTGCT), *ldhA*, and *aiiA*—were independently inserted into vector pET-*P_{luxI}* at *Eco*RI/*Hind* III, *Bam*HI/*Eco*RI, and *Hind*III/*Xho*I sites, resulting in vectors pET-*P_{luxI}*:*egfp*, pET-*P_{luxI}*:*ldhA*, and pET-*P_{luxI}*:*aiiA*, respectively. The *aiiA* gene tailored for AHL degradation was cloned from *B. thuringiensis*.

To determine the effects of AiiA on *egfp* expression and lactic acid production, its coding gene *aiiA* was equipped with a moderate strength of RBS (AAGTTAAGAGGC AAGA) and then inserted into vectors pET-*P_{luxI}*:*egfp* and pET-*P_{luxI}*:*ldhA* at *Hind* III/*Xho* I sites, resulting in vectors pET-*P_{luxI}*:*egfp-aiiA* and pET-*P_{luxI}*:*ldhA-aiiA*, respectively. To vary *aiiA* expression, the *aiiA* gene with weak or strong RBS (weak: CACCATACACTG; strong: AAG GAGGTTTGGA) was independently inserted into vector pET-*P_{luxI}*:*ldhA* at *Hind* III/*Xho* I sites, leading to vector pET-*P_{luxI}*:*ldhA-aiiA*(weak) and pET-*P_{luxI}*:*ldhA-aiiA*(strong), respectively. After the above vectors were independently transformed into competent *E. coli* Δ *ldhA* cells, we obtained seven recombinant strains named Q01, Q02, Q03, Q04, Q05, Q06, and Q07 (Table S1). To exploit AHL for coordinated gene expression, the vector pluxIR was transformed into above seven recombinant strains, resulting in recombinant strains Q11, Q12, Q13, Q14, Q15, Q16, and Q17, respectively. The control strains were constructed using empty pET- and pACYC-series vectors, including C01, C02, C03, C04, and C05. We expected that the strains overexpressing AHL synthesis gene exhibited “ON” state, while the strain coexpressing AHL synthesis and degradation gene manifested “ON to semi-OFF” state. All primers are listed in Table S2.

SDS-PAGE analysis

To determine whether the engineered QS cassette functioned properly in *E. coli*, the strains were independently inoculated in 250 mL shake-flasks, each containing 100 mL Luria-Bertani medium and antibiotics as appropriate. After 3 h cultivation, 0.5 mM IPTG was added to induce protein expression. After 16 h shaking cultivation at 150 \times g and 37 °C, cells were harvested by centrifugation at 7379 \times g for 10 min, and then mixed with 4 \times SDS-polyacrylamide gel electrophoresis (SDS-PAGE) loading buffer and boiled for 5 min. Protein expression was analyzed by 12% (w/v) SDS-PAGE with cell-free extract under denaturing conditions. Mini-Protein



III Electrophoresis System (Bio-Rad, USA) was used to perform this operation. Coomassie Brilliant Blue R-250 (0.2%, w/v) was used to stain proteins on the gel, and protein concentration was measured by Bradford method with bovine serum albumin (BSA) as standard protein (Table S3).

Determination of relative fluorescence

To investigate eGFP expression, strains were grown in shake-flasks at 37°C. Samples were taken every 2 h from 0 to 46 h, and 200 μ L fermentation broth was added into a 96-well microtiter plate (Corning, NY, USA). To avoid fluorescence quenching, samples were stored in the dark at 4°C before the instrument was ready. Fluorescence intensity was measured using the Enspira microplate reader (PerkinElmer, Singapore) at 485 nm excitation wavelength and 9.5 mm measurement height. Relative fluorescence intensity was defined as the fluorescence value divided by OD_{600} .

Microscopic observation of fluorescence

To directly view eGFP expression, strains were independently cultivated in shake-flasks, and fermentation broth was sampled at 8 h, 20 h, and 32 h and stored in the dark at -20 °C before the microscope was ready. For microscopic observation, 30 μ L sample was added on a microscope slide (Thermo Fisher Scientific, MA, USA), and an equal volume of a mixture containing glycerol and phosphate buffer saline (PBS) at pH 7.4 was used as a sealant, which was under a cover glass without air bubble. Leica SP8 laser scanning confocal microscopes using Leica DMC2900 imaging system (Leica, Wetzlar, Germany) was set to eGFP mode with 40 \times objective and scale bar of 20 μ M.

Enzyme activity assay

To measure the LdhA activity of Q12, Q15, Q16, and Q17, broths were sampled at different time points (8 h, 14 h, 20 h, 32 h, and 48 h), and then centrifuged at 7379 \times g for 10 min. The harvested cells were washed

twice using 100 mM PBS (pH 6.5), and then sonicated and centrifuged at $10,625\times g$ for 10 min. Proteins were quantified using Bicinchoninic acid (BCA) assay kit (Bioroyee, Beijing, China). 20 μ L supernatant was mixed with 200 μ L BCA assay solution and incubated at 60°C for 30 min. When the mixture was cooled to room temperature, absorbance at 570 nm was measured using a microplate reader. The LdhA activity was determined by lactate dehydrogenase (LDH) kit (Beijing Xinhualvyan Science and Technology, Beijing, China), which can spectrophotometrically analyze the decrease rate of absorbance at 340 nm corresponding to NADH oxidation at 37°C. This decrease rate is named as $\Delta A/\text{min}$. The reaction mixture consisted of 0.05 mL supernatant, 2.0 mL LDH assay solution, and 0.2 mL pyruvate solution. After pyruvate solution was added into the reaction mixture, enzyme activity was immediately measured. The specific activity formula is $\text{LdhA}(\text{U}/\text{mg}) = \Delta A/\text{min} * (106/6220) * (2.25/0.05) / \text{protein concentration} = \Delta A/\text{min} * 7235 / \text{protein concentration}$, and the molar extinction coefficient is $6220 \text{ M}^{-1} \text{ cm}^{-1}$ at 340 nm.

Determination of relative transcriptional levels

To clarify how the “ON” mode of LdhA expression affected glycolysis and glucose phosphotransferase system (PTS) and to confirm the AiiA expression under different strength of RBS, qRT-PCR was performed. The strain Q12 and the reference strains C01 and C02 were sampled at different time points and harvested by centrifugation. RNA was isolated using QIAamp RNA Blood Mini Kit (Qiagen, Duesseldorf, Germany). The same RNA extraction was also performed for Q15, Q16, and Q17. After RNase-free DNase was added, cDNA was synthesized through SuperScript III Reverse Transcriptase (Invitrogen, CA, USA). Next, qRT-PCR analysis was carried out using the resultant cDNA by ABI ViiA 7 Real-Time PCR System (Thermo Fisher Scientific, MA, USA). The 16S rRNA coding gene was used as the control to determine the relative expression levels of genes *ldhA*, *gapA*, *gapC*, *ptsH*, *ptsI*, *pykF*, and *aiiA*.

Analytical methods

Cell concentration was determined by microplate reader at 600 nm with 200 μ L fermentation broth added in a cuvette. The fermentation broth was centrifuged at $10,625\times g$ for 10 min, and the supernatant was filtered through a 0.22- μ M PES membrane. Metabolites including lactic acid and acetic acid were measured by a high-performance liquid chromatography (HPLC) system (Shimazu, Kyoto, Japan) equipped with a C_{18} column and an SPD-20A UV detector at 210 nm. Column temperature was maintained at 25 °C, and the mobile phase was 0.05% phosphoric acid at a flow rate of 0.8 mL

min^{-1} . Injection volume was 20 μ L. Glucose and L-lactic acid were measured by SBA-40E biosensor (Shandong, China). The reaction and cleaning time were 20 s and 10 s, respectively. The injection volume was 25 μ L. D-lactic acid is the total lactic acid minus L-lactic acid.

To analyze AHL and its derivatives, cell-free supernatant was extracted with acidified ethyl acetate (by 0.05% formic acid). The extraction was performed in triplicate, and mixture was evaporated to dryness. The extract was dissolved in methanol, filtered through a 0.45- μ m organic membrane and followed by UPLC-MS/MS analysis (Waters ACQUITY UPLC/Quattro Premier, USA, Massachusetts). A Waters ACQUITY SDS C_{18} column was utilized as the solid phase and maintained at 45°C. Mobile phase consists of 0.1% acetic acid (A) and acetonitrile (B). Gradient elution was conducted with the profile of 99% A at the first 1 min, 40% A from 2 to 4 min, 100% B from 5 to 8 min, 100% B from 9 to 11 min, and 99% A from 12 to 13 min. Flow rate was 0.3 mL/min. Mass detection was performed in ES+ ionization mode and data were analyzed by Masslynx V4.1 software.

Characterization of recombinants

In this study, QS was exploited to coordinate cell growth and lactic acid production in *E. coli*. In doing so, we constructed two vectors carrying different resistance genes and replicons. The medium-copy vector, pluxIR, carries *luxI-luxR* gene cluster to automatically synthesize AHL and constitutively express AHL-binding protein LuxR (Fig. 1B). The high-copy vector pET- P_{luxI} harbors a P_{luxI} promoter and a pET-28a(+) backbone, where gene expression is controlled by QS. Due to this architecture, the vector pluxIR could express LuxR-AHL, which in turn induced the expression of gene on vector pET- P_{luxI} . With the increase of cell density, the transcriptional regulator LuxR-AHL would bind P_{luxI} promoter and elicit the transcription of downstream gene. Apart from this inducible expression, the QS-based “ON to semi-OFF” expression was realized by using pluxIR and pET- $P_{luxI}:aiiA$, where the *aiiA* gene was inserted downstream of the P_{luxI} promoter on vector pET- P_{luxI} . Since pluxIR was used to express the LuxR-AHL complex which in turn initiated the transcription of *aiiA* on vector pET- $P_{luxI}:aiiA$, the resulting AiiA would repress the transcription of P_{luxI} promoter-driven *luxI* and *aiiA* due to AiiA-mediated AHL degradation, therefore leading to “OFF” state. Notably, this “OFF” state was transient because AiiA expression was rapidly turned off. When AiiA concentration decreased to a threshold at which AHL could not be completely degraded, QS was then turned on and gene expression was restarted. The above architecture was designated as “ON to semi-OFF”. In such an architecture, the LuxR-AHL complex activated gene transcription and

thereby led to constant “ON” state (Fig. 1). By contrast, the combination of LuxR-AHL and AiiA triggered not only AHL synthesis but also its degradation, leading to “ON to semi-OFF” state (Fig. 1).

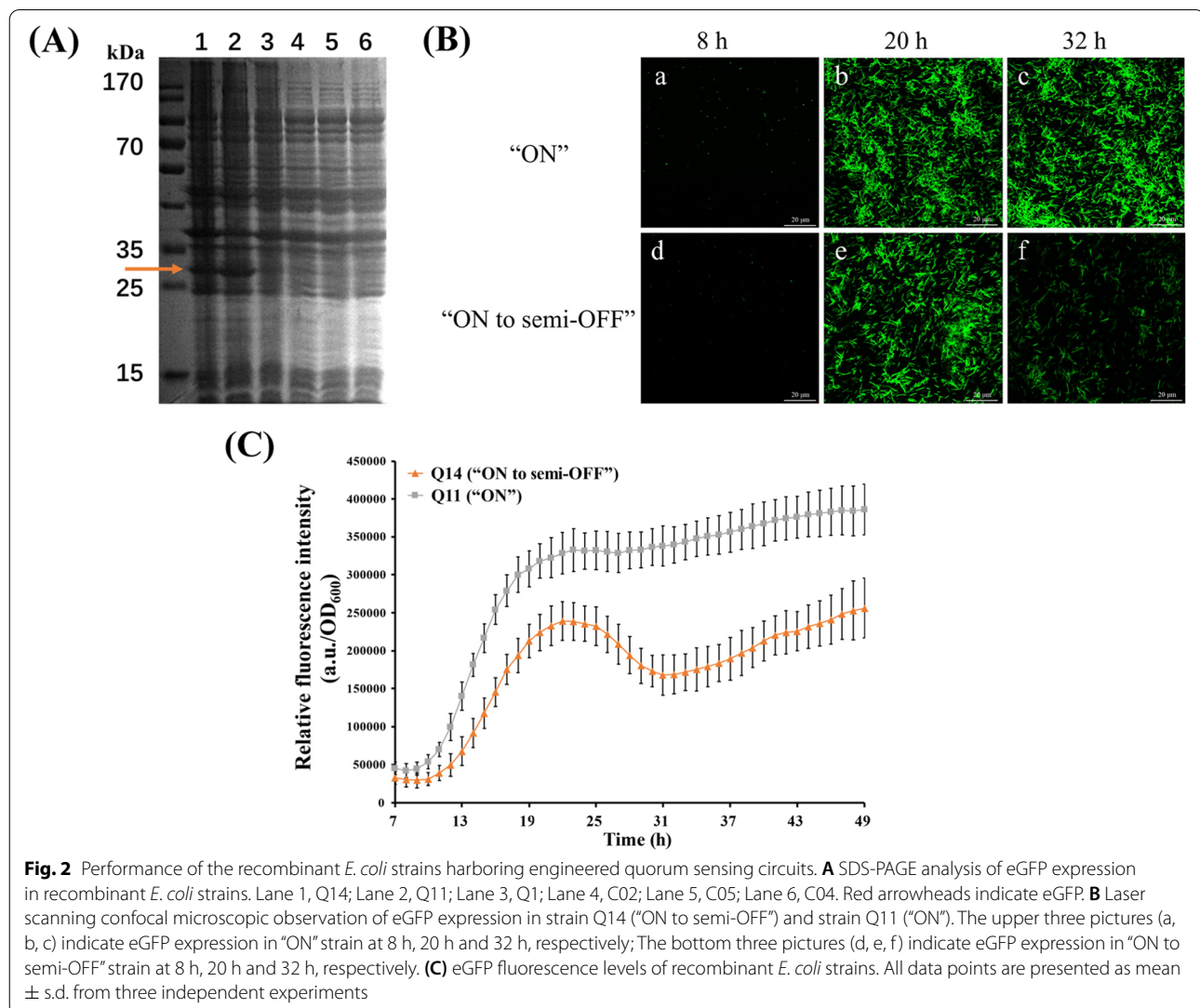
This engineered system would dynamically control the expression of gene downstream of P_{luxi} promoter on vector pET- P_{luxi} or the gene between P_{luxi} promoter and *aiiA* gene on vector pET- P_{luxi} :*aiiA* where the transcription initiation of target gene is earlier than *aiiA* gene. RBS was inserted upstream of *aiiA* to allow *aiiA* and target gene sharing a cassette. To test the two engineered QS circuits, eGFP was employed as the reporter (Fig. 1, strain A and B). To confirm the QS circuits, *egfp* was replaced by *ldhA* (Fig. 1, strain C and D). To exclude the influence of native *ldhA* gene on QS circuits, it was deleted from *E. coli* genome through λ Red recombination method. To do so, three vectors, viz, pkD13, pkD46, and pCP20 were used

(Table S1). The vector, pkD13, was used as PCR template including FRT, kanamycin resistance gene, and homology arms of *ldhA* gene. After pkD46 and PCR products were electro-transformed into strains, the resulting colonies were screened by kanamycin plates. Next, vector pCP20 was transformed into positive clones, and kanamycin resistance gene was eliminated. Positive clones were screened by colony PCR, and *ldhA* mutant was acquired (Fig. 2B). All plasmids and mutants were confirmed by DNA sequencing. The primers used for PCR amplification are shown in Table S2.

Results

Performance of eGFP

Compared with Green Fluorescent Protein (GFP), eGFP manifests stronger fluorescence and has been widely used for protein labeling. The plasmids pET- P_{luxi} :*egfp* and



pET-*P_{luxi}*-*egfp-aiiA* were constructed for gene expression in “ON” and “ON to semi-OFF” mode, respectively. To examine the “ON” mode, the strain Q11 was incubated in M9 medium. After centrifugation at 10,625 x g and resuspension with PBS, the “ON” strain demonstrated clear yellow-green light, whereas the control strains, Q01 and C02 did not (Fig. S1). This pre-experiment confirmed that the “ON” mode could trigger reporter gene expression. Next, we investigated the “ON to semi-OFF” strain Q14. As shown by the lane 1 and lane 2 in Fig. 2A, two significant bands exhibited molecular weight similar to eGFP (approximately 26.9 kDa), and the band in lane 2 was larger than that in lane 1, suggesting that eGFP was properly expressed in *E. coli*Δ*ldhA*, and its expression level in “ON” strain was higher than that in “ON to semi-OFF” strain. No significant band similar to eGFP was observed in lane 3, lane 4, lane 5, and lane 6 of the control groups (Fig. 2A), indicating that an intact QS circuit is required for driving eGFP expression.

To determine how long eGFP expression lasted, Q14 (“ON to semi-OFF”) and Q11 (“ON”) were cultivated and observed using a laser scanning confocal microscope (Fig. 2B). Results showed that both “ON to semi-OFF” and “ON” strains did not show fluorescence at 8 h (Fig. 2B, picture *a* and *d*), with a significant increase at 20 h (Fig. 2B, picture *b* and *e*). The “ON” strain showed continuous increase of fluorescence level from 20 to 32 h and eventually exceeded “ON to semi-OFF” strain (Fig. 2B, picture *e*, *f*, and *c*). Unlike “ON” strain, the “ON to semi-OFF” strain showed decline of fluorescence from 20 h to 32 h (Fig. 2B, picture *b* and *c*). To precisely determine eGFP expression, we investigated the relative fluorescence levels (fluorescence/OD₆₀₀). As shown in Fig. 2C, the “ON” strain manifested high relative fluorescence and maintained it till 49 h. This constant eGFP expression was induced by the accumulating AHL. Unlike “ON” strain, the “ON to semi-OFF” strain manifested less fluorescence. In particular, its relative fluorescence level was increasing until 22 h and then decreasing, which was possibly due to AHL degradation by AiiA. This decrease of fluorescence level lasted until 34 h, and then maintained a relatively stable state called “semi-OFF”. Such a state might be ascribed to incomplete AHL degradation. To confirm this prediction, UPLC-MS/MS was used to monitor AHL (3-oxo-C6-HSL) and its derivative (ring opening of 3-oxo-C6-HSL) in the broth of Q14 (Supplementary

Fig. 2D). The molecular ion ([M+H]⁺=214.10, 232.11) peaks were recorded by UPLC-MS. The peak of 214.10 at 3.49 min was further analyzed by tandem mass spectrometry (MS/MS) and then recorded two ion fragment ([M+H]⁺=102.05, 113.06) peaks, suggesting that these peaks belong to AHL (3-oxo-C6-HSL). The existing AHL and their ring opening derivatives in broth indicated that QS-controlled AiiA could not completely degrade AHL and thereby failed to completely shut down eGFP expression, leading to “semi-OFF” state.

Performance of the recombinant strains overexpressing *ldhA*

Given that the two QS circuits (“ON” and “ON to semi-OFF”) worked properly in *E. coli*, we next applied them to regulate *ldhA* expression. To evaluate LdhA expression, we measured the specific activity of LdhA in Q12 (“ON”) and Q15 (“ON to semi-OFF”). We found that the LdhA specific activity of Q15 increased in the first 20 h and then remarkably decreased, while that of Q12 increased in this first 32 h and then slightly decreased (Fig. 3A). Clearly, the fluctuation of LdhA specific activity was roughly consistent with the expression level of eGFP shown in Fig. 2B. Moreover, the *ldhA*-overexpressing “ON” strain entered the logarithmic growth phase slowly, with OD₆₀₀ of 0.205 at 10 h, but its maximum OD₆₀₀ was 0.722 which was only lower than the strain harboring empty vector (Fig. 3B). In contrast, the “ON to semi-OFF” strain showed a shorter lag phase and lower growth rate compared to the “ON” strain. This “ON to semi-OFF” strain presented an OD₆₀₀ value similar to the strain harboring empty vector in the first 8 h, and this OD₆₀₀ value was exceeded by the “ON” strain at 16 h. As for glucose consumption, except for the strains harboring empty vector, all other strains did not demonstrate a significant difference in the first 6 h (Fig. 3C). This finding is consistent with lag phase growth, and the glucose consumption of Q12 was higher than that of C02, C01, and “ON to semi-OFF” strains. Furthermore, the strain Q12 exhibited 0.1163 g h⁻¹ of glucose consumption, which is the highest except for the strains harboring empty vector.

Given the increase of growth rate and glucose consumption of Q12, we speculated that QS-dependent dynamic regulation of *ldhA* expression might affect glucose metabolism. Quantitative real-time PCR was thus conducted to determine the relative transcriptional levels

(See figure on next page.)

Fig. 3 Shake-flask cultivation of the recombinant *E. coli* strains. **A** Comparison of LdhA specific activities in two different mode strains that Q12 and Q15. **B** Cell growth in shake flask of strains. **C** Glucose consumption in shake flask. **D** Gene transcription of the strain overexpressing *ldhA* by “ON” mode. *ldhA*, D-lactate dehydrogenase coding gene; *gapA* and *gapC*, GAPDH coding genes; *ptsH*, PTS phosphocarrier protein coding genes; *ptsI*, PTS enzyme I coding gene; *pykF*, pyruvate kinase coding gene. **E** Comparison of gene transcription in Q12 upon 12 h and 22 h seed culture. **F** D-lactic acid. **G** Acetic acid. All data are presented as mean ± s.d. from three independent experiments. The statistical analysis is based on Mann-Whitney *U* test. **P* < 0.05 and ***P* < 0.01

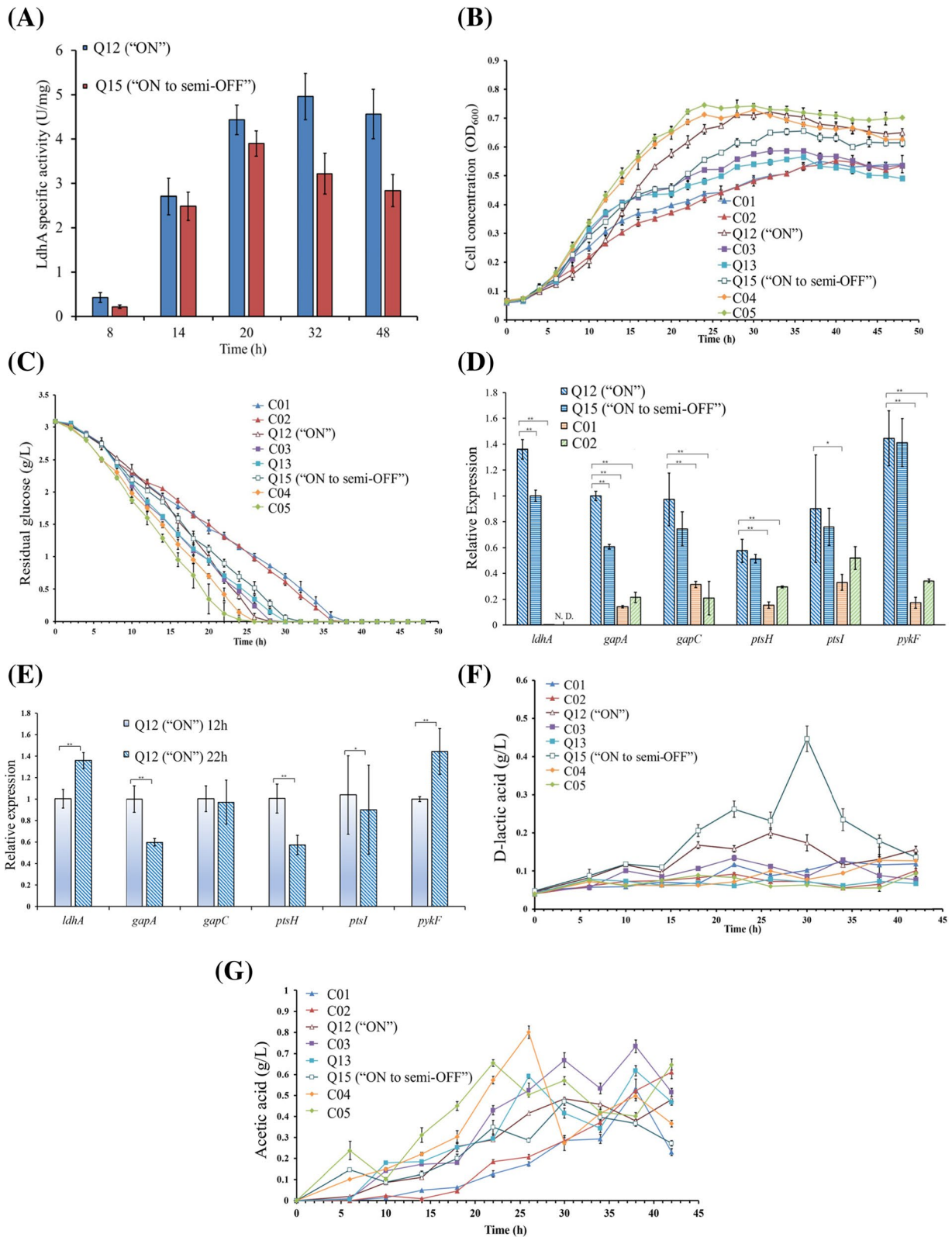


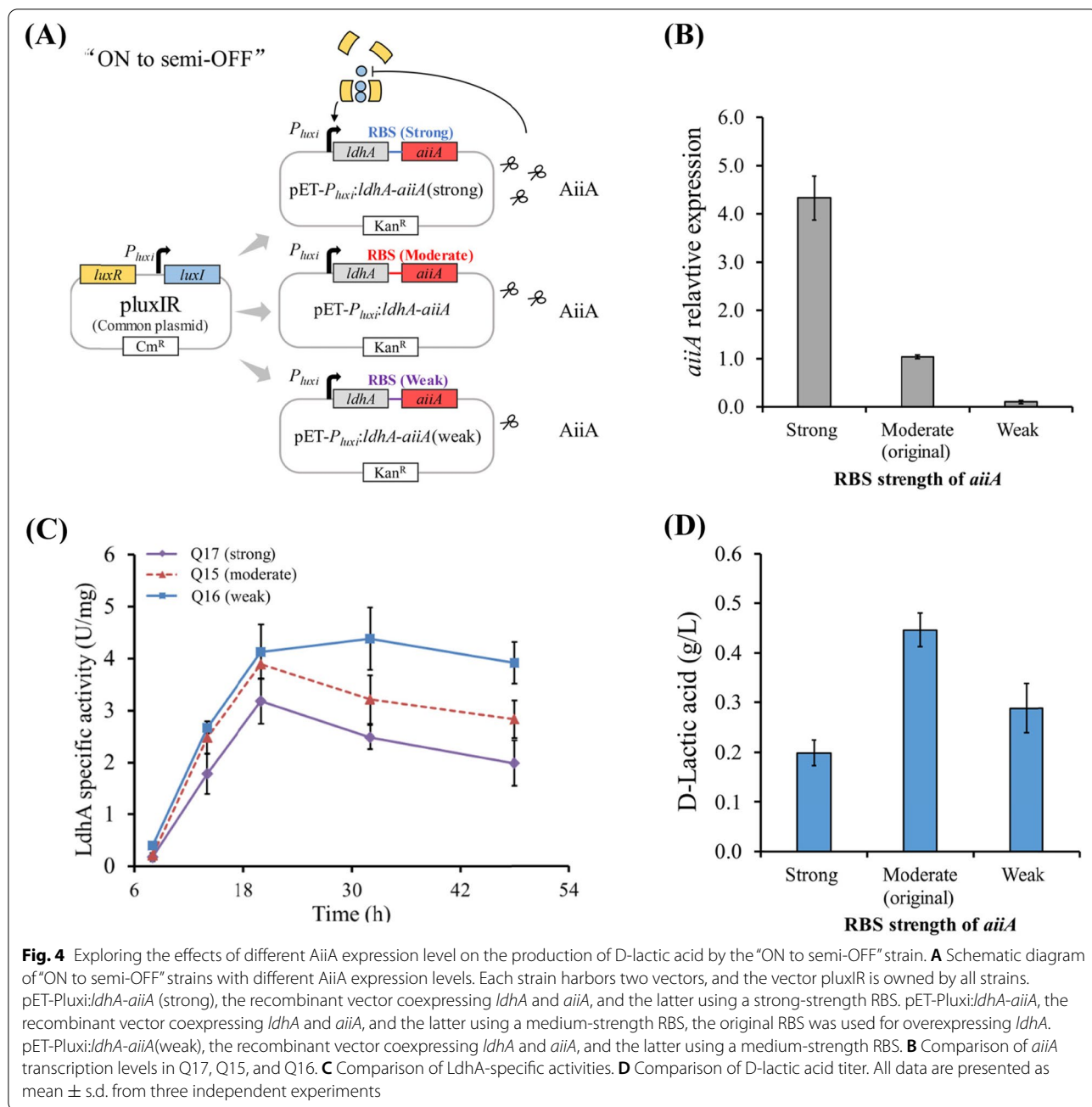
Fig. 3 (See legend on previous page.)

of key enzyme genes related to glucose utilization. The key enzyme genes include *ptsH* and *ptsI* that encode enzyme I (EI) and histidine phosphocarrier protein (Hpr) in PTS, respectively, and the genes that encode pyruvate kinase I (PykF) and glyceraldehyde-3-phosphate dehydrogenase (GAPDH, an isoenzyme of GapA and GapC). PykF and GAPDH are key for *E. coli* glycolysis. As shown in Fig. 3D, almost all examined genes in strains Q12 and Q15 displayed enhanced transcription compared to those in control strains ($*P < 0.05$ and $**P < 0.01$), suggesting that the LdhA expression in “ON” and “ON to semi-OFF” strains activated PTS system and glycolysis, which therefore accelerated glucose uptake. This might compensate the decreased cell growth due to production formation in lag phase. Apart from the above experiments, we also investigated the gene expression of Q12 and Q15 at 12 h and 22 h. Results showed that the genes *ldhA* and *pykF* in both Q12 and Q15 were up-regulated from 12 h to 22 h, while other genes in Q12 were down-regulated (Fig. 3E), indicating that QS-mediated *ldhA* expression significantly up-regulated the key enzyme genes related to glycolysis and PTS system in a non-proportional way.

Furthermore, we investigated the formation of acids under QS-based dynamic control. As shown in Fig. 3F, the *ldhA* mutants harboring vector pluxIR (for AHL synthesis) but without overexpressing *ldhA* produced less D-lactic acid, as compared with the *ldhA* mutants overexpressing both AHL synthesis gene and *ldhA*. For the reference strains, the *ldhA* mutant strain C05 produced only 28.23% D-lactic acid as compared to the strain C04, indicating that *ldhA* was key for D-lactic acid production. To determine whether *ldhA* was solely controlled by the engineered QS circuit, *ldhA* was deleted from the *E. coli* genome but inserted into downstream of QS promoter, leading to vector pET-*P_{luxI}:ldhA*, or inserted between the promoter and *aiiA* gene, resulting in vector pET-*P_{luxI}:ldhA-aiiA*. The corresponding recombinant strains were named Q12 and Q15, respectively. We found that Q15 (“ON to semi-OFF”) produced more D-lactic acid, and presented the highest yield and space-time yield compared with Q12 (“ON”) and the control strains. In addition, while the strain Q12 (“ON”) presented 0.2295 g/L of maximum yield and 0.005526 g/h/L of space-time yield, the strain Q15 (“ON to semi-OFF”) presented 0.4464 g/L of maximum yield and 0.01488 g/h/L of space-time yield, which were 94.5% and 169.2% increase in maximum yield and space-time yield, respectively, as compared with Q12 (“ON”). Surprisingly, compared with the “ON” strain Q12, the “ON to semi-OFF” strain Q15 demonstrated 2.3-fold increase in maximum D-lactic acid titer. As the main byproduct in lactic acid production, acetic acid occupies a lot of carbon flux from pyruvate. As shown in Fig. 3G, acetic acid formation was

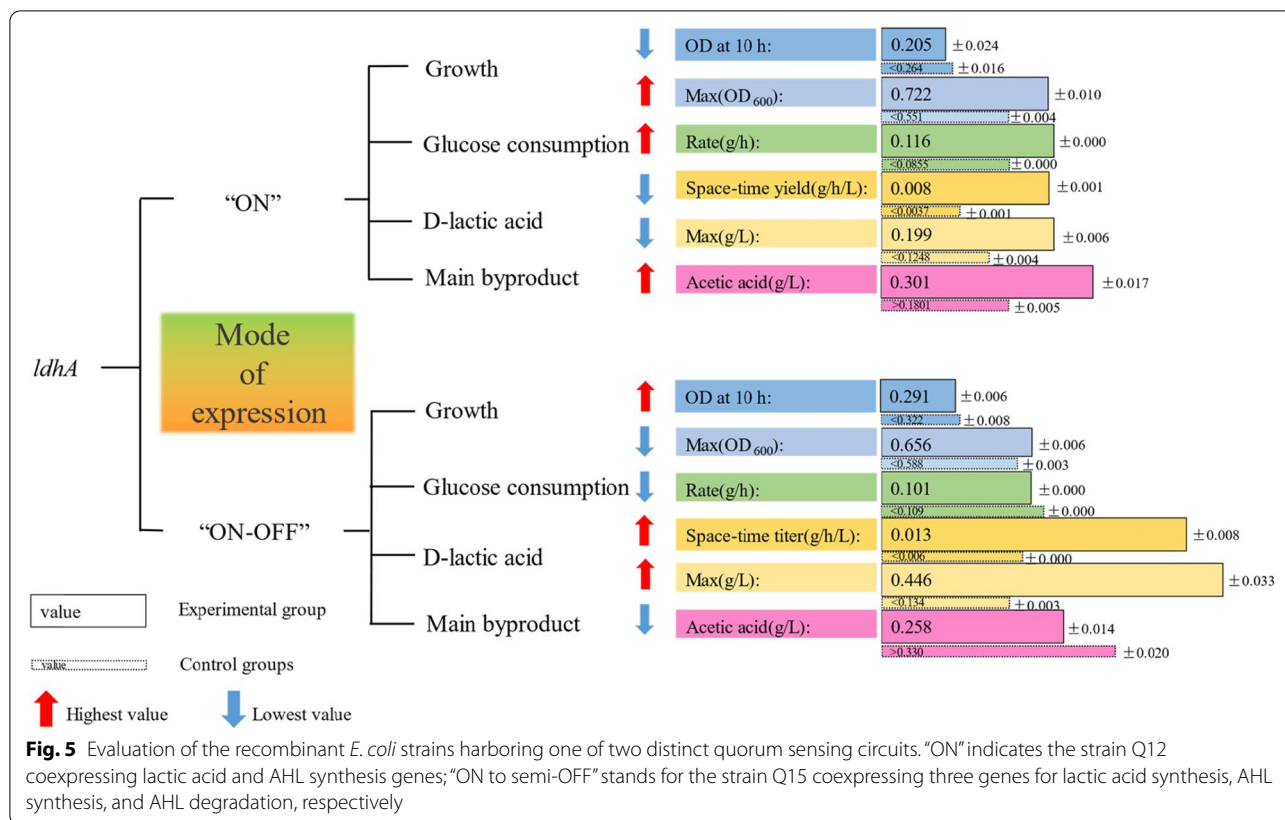
associated with growth conditions, and Q12 and Q15 showed similar fluctuation in levels of acetic acid and D-lactic acid.

Given that the “ON to semi-OFF” strain outperformed “ON” strain in the production of lactic acid (Fig. 3F), we next ameliorated the tunability of “ON to semi-OFF” circuit and investigated its impact on lactic acid production. Since AiiA degrades AHL, we conjecture that the transcription level of *aiiA* might affect QS-mediated “On” and “Off” of gene expression. Moreover, considering ribosome binding site (RBS) markedly affects transcription (Salis et al. 2009; Pflieger et al. 2006), we adjusted the AiiA expression level by altering RBS. In doing so, two distinct RBS, which are respectively stronger and weaker than the previously validated *aiiA* RBS in vector pET-*P_{luxI}:ldhA-aiiA* (Levin-Karp et al. 2013), were separately inserted the upstream of *aiiA* gene, leading to two recombinant plasmids pET-*P_{luxI}:ldhA-aiiA*(strong) and pET-*P_{luxI}:ldhA-aiiA*(weak), respectively. Afterwards, the two recombinant plasmids were separately co-transformed with vector pluxIR into *E. coli*, leading to two “ON to semi-OFF” strains named Q17 and Q16 (Fig. 4A). The two “ON to semi-OFF” strains were compared with the aforementioned strain Q15. Real-time PCR showed that after 30 h cultivation, the transcription level of the strain Q17 was 4.2 and 40.9 times that of the control strains Q15 and Q16, respectively (Fig. 4B), indicating that RBS positively affected *aiiA* transcription. To disentangle the impact of *aiiA* transcription on *ldhA* expression, the aforementioned three strains were investigated for their LdhA activity. As shown in Fig. 4C, in the first 20 h, all three strains showed rapid increase in LdhA activity, and the enhancement in descending order was Q16, Q15, and Q17. These results suggested that QS system manifested “ON” state, and *ldhA* was rapidly expressed. Notably, the strain Q16 showed the highest level of *ldhA* expression (Fig. 4C). After 20 h cultivation, the strains Q15 and Q17 showed a decline in LdhA activity, and the latter strain exhibited lower LdhA activity. Interestingly, the LdhA activity of strain Q16 did not decline until 32 h. These results suggested that after 20 h cultivation the strain employing moderate or strong *aiiA* RBS showed a decrease in LdhA activity because the expressed AiiA repressed the QS-driven *ldhA* expression earlier, and QS was switched to “semi-OFF” state. By contrast, the strain employing weak *aiiA* RBS showed LdhA degradation after 32 h, which was similar to the behavior of “ON” strain, indicating that the QS circuit employing weak *aiiA* RBS was less switched to “semi-OFF” state compared to the QS circuit employing moderate or strong *aiiA* RBS. Lastly, we investigated D-lactic acid formation at 30 h (Fig. 4D). Compared with reference strain *E. coli* (Δ *ldhA*/pET-*P_{luxI}:ldhA-aiiA*/pluxIR), the strains Q17 and Q16 demonstrated 55.6% and 35.2% decrease in the production



of D-lactic acid, respectively. These results indicated that the transcriptional up-regulation of *aiiA* led to a significant decrease in *ldhA* expression and lactic acid formation. On the other hand, the transcriptional down-regulation of *aiiA* resulted in a transcription level of *ldhA* similar to the "ON" state, which also constrained D-lactic acid formation. Taken together, the "ON to semi-OFF" outperformed "ON" in the production of D-lactic acid, as it demonstrated moderate *aiiA* transcription.

Lastly, we systematically assessed the performance of "ON" and "ON to semi-OFF" strains in cell growth, glucose consumption, and production of D-lactic acid and byproducts. The "ON" strain consumed more glucose and grew faster, while the "ON to semi-OFF" strain produced less acetic acid (byproduct) but more D-lactic acid (Fig. 5). In other words, the QS-based "ON" and "ON to semi-OFF" strains have their pros and cons in dynamic regulation of LdhA expression.



Discussion

Microbial production of D-lactic acid suffers growth inhibition due largely to overexpression. Dynamic regulation of gene expression can mitigate metabolic stress (Xu et al. 2014; Zhou et al. 2012). QS represents a typical dynamic gene regulation. Inspired by this, we engineered two recombinant *E. coli* strains harboring QS circuits. The "ON" strain harbors the expression cassette *ldhA-LuxIR* for the production of both lactic acid and AHL, while the "ON to semi-OFF" strain harbors both *ldhA-luxIR* and *aiiA* gene for the production of not only lactic acid and AHL but also AiiA which is an enzyme for AHL degradation (Fig. 1). Compared with the strain without LuxI-LuxR cassette, the "ON" strain coexpressing LuxI-LuxR and *ldhA* showed 83.6% and 31.0% increase in growth rate and OD₆₀₀, respectively (Fig. 3). Although the "ON to semi-OFF" strain grew slower than "ON" strain, it demonstrated a higher titer and productivity of D-lactic acid (Fig. 5). Compared with the reference strain harboring only *ldhA* gene in vector, both the "ON" and "ON to semi-OFF" strains demonstrated synchronization between cell growth and D-lactic acid production. Although there exists a native LuxS/auto-inducer 2 (AI-2) system in *E. coli*, which regulates cell density via AI-2 (Surette and Bassler, 1998), however, our

experiment showed that the promoter *P_{luxI}* did not work in the absence of LuxI and LuxR. The above results indicated that QS can be exploited to coordinate cell growth and product formation. Compared with the "ON" strain, the "ON to semi-OFF" strain seems to be more appropriate for the production of lactic acid.

Active cell growth is a prerequisite for high-level production of desired metabolites. In this study, both "ON" and "ON to semi-OFF" strains showed enhanced cell growth when compared with the reference strain without the engineered QS circuit. This was primarily attributed to QS-dependent dynamic regulation of *ldhA* expression. Since LdhA catalyzes pyruvate to D-lactic acid, the excessive D-lactic acid leads to growth inhibition (Wang et al. 2018). The "ON" strain mitigated acid stress through the intensification of PTS and glycolysis, which thereby benefited cell growth. *E. coli* stringently controls lactic acid synthesis. Despite up to 5.55×10^4 -fold increase in the relative expression of LdhA (Fig. 3D), only limited lactic acid was produced (Fig. 3F). By contrast, the QS-based "ON to semi-OFF" strain showed improved production of D-lactic acid. This was ascribed largely to the switch of *ldhA* expression from "On" to "partial Off", thereby constraining acetic acid production (Fig. 3G). Compared with static

strategies to coordinate cell growth and product formation, this QS-dependent dynamic strategy relies on timely sensing of cell density, and thus is appropriate for modulating the formation of metabolites especially those toxic to cells.

In this study, both “ON” and “ON to semi-OFF” strains produced a small amount of D-lactic acid (Figs. 3F, 4D, and 5). The reasons may be the follows: (1) vectors imposed heavily on host cell due to consumption of cellular resources; (2) the AHL-inducible P_{luxi} is a weaker promoter compared to T7, *tac* and *lac* promoters; and (3) fermentation conditions were not optimized. To boost D-lactic acid production, the following may be considered. First, to minimize plasmid burden, the genes for AHL synthesis and degradation could be integrated into host genome, and only *ldhA* gene is left in vector. Second, tandem repetitive P_{luxi} promoter could be employed to intensify LdhA expression and thereby divert pyruvate to D-lactic acid. Third, fermentation conditions including carbon source, nitrogen source, pH value, and dissolved oxygen could be systematically optimized. Finally, acid stress should be attenuated. To achieve this, in situ recovery of D-lactic acid from fermentation broth could be implemented. In addition, feedback inhibition could be minimized by engineering gene circuit (Kelly et al. 2018) or recruiting feedback inhibition-insensitive enzymes (Chen et al. 2014; Takpho et al. 2018).

Cell tolerance is usually controlled by multiple genes. CRISPR tools, especially CRISPR interference (CRISPRi), can be used to improve cell tolerance (Wang et al. 2019; Xu et al. 2019), as sgRNA array can lead dCas9 to multiple genes (Bikard et al. 2013). It has been shown that sgRNAs can be designed and synthesized to target multiple lactic acid pathways (Wang et al. 2018). CRISPRi can also regulate gene expression when combined with other tools. Indeed, microbes have bridged the gap between QS and CRISPR-Cas system. For instance, wild-type *Pseudomonas aeruginosa* recruits QS to govern CRISPR-Cas adaptive immune system (Patterson et al. 2016; Høyland-Kroghsbo et al., 2017), indicating the intrinsic connection between QS and CRISPR system. Inspired by this rationale, a pathway-independent genetic control module was constructed by linking QS to CRISPR. This engineered module can dynamically modulate gene expression (Gupta et al. 2017). More broadly, when this QS-based module was linked to metabolite sensor, a two-layered regulatory circuit was engineered (Doong et al. 2018). Apart from CRISPRi, RNAi can also be linked to QS circuit for dynamic control of the metabolic pathways in eukaryotes (Williams et al. 2015). Since QS is common in both bacteria and fungi, the method developed in the present study could prove useful for metabolic engineering of other species as well.

Conclusions

To coordinate cell growth and lactic acid synthesis in *E. coli*, we constructed two QS-based strains: one strain overexpressing AHL synthesis genes (“ON”), the other strain overexpressing both AHL synthesis and degradation gene (*aiiA*) (“ON to semi-OFF”). Compared to the reference strain harboring only *ldhA* gene in vector, both “ON” and “ON to semi-OFF” strains showed synchronization between cell growth and D-lactic acid production, indicating that QS can be exploited to coordinate cell growth and product formation.

Acknowledgements

We thank Dr. ZHAO Peng for his assistance in material preparation.

Authors' contributions

C. G. and P. T. conceived and designed research. C. G., S. R., and H. J. conducted experiments. C. G. analyzed data. P. T. wrote the manuscript. The authors read and approved the final manuscript.

Funding

This study was funded by grants from the Hebei Project for Development of Science and Technology Guided by Central Universities (206Z2902G), National Key Research and Development Program of China (2018YFA0901800), and Project of Beijing Municipal Commission of Education (KZ201911417049).

Availability of data and materials

The data are available from the corresponding author on a reasonable request.

Declarations

Ethics approval and consent to participate

This article does not contain any studies with human participants or animals performed by any of the authors.

Consent for publication

All authors approved the publication of this manuscript.

Competing interests

The authors declare that they have no competing interests.

Received: 23 August 2021 Accepted: 5 January 2022

Published online: 26 January 2022

References

- Balestrino D, Haagensen JA, Rich C, Forestier C (2005) Characterization of type 2 quorum sensing in *Klebsiella pneumoniae* and relationship with biofilm formation. *J Bacteriol* 187(8):2870–2880
- Bikard D, Jiang W, Samai P, Hochschild A, Zhang F, Marraffini LA (2013) Programmable repression and activation of bacterial gene expression using an engineered CRISPR-Cas system. *Nucleic Acids Res* 41(15):7429–7437
- Bunch PK, Mat-Jan F, Lee N, Clark DP (1997) The *ldhA* gene encoding the fermentative lactate dehydrogenase of *Escherichia coli*. *Microbiology* 143(1):187–195
- Chen Z, Bommarreddy RR, Frank D, Rappert S, Zeng A-P (2014) Dereglulation of feedback inhibition of phosphoenolpyruvate carboxylase for improved lysine production in *Corynebacterium glutamicum*. *Appl Environ Microbiol* 80(4):1388–1393
- Datsenko KA, Wanner BL (2000) One-step inactivation of chromosomal genes in *Escherichia coli* K-12 using PCR products. *Proc Natl Acad Sci USA* 97(12):6640–6645
- Din MO, Danino T, Prindle A, Skalak M, Selimkhanov J, Allen K, Julio E, Atolia E, Tsimring LS, Bhatia SN (2016) Synchronized cycles of bacterial lysis for *in vivo* delivery. *Nature* 536(7614):81–85

- Dinh CV, Prather KL (2019) Development of an autonomous and bifunctional quorum-sensing circuit for metabolic flux control in engineered *Escherichia coli*. *Proc Natl Acad Sci USA* 116(51):25562–25568
- Dong YH, Xu JL, Li XZ, Zhang LH (2000) AiiA, an enzyme that inactivates the acylhomoserine lactone quorum-sensing signal and attenuates the virulence of *Erwinia carotovora*. *Proc Natl Acad Sci USA* 97(7):3526–3531
- Dong YH, Wang LH, Xu JL, Zhang HB, Zhang XF, Zhang LH (2001) Quenching quorum-sensing-dependent bacterial infection by an N-acyl homoserine lactonase. *Nature* 411(6839):813–817
- Dong YH, Gusti AR, Zhang Q, Xu JL, Zhang LH (2002) Identification of quorum-quenching N-acyl homoserine lactonases from *Bacillus* species. *Appl Environ Microbiol* 68(4):1754–1759
- Doong SJ, Gupta A, Prather KL (2018) Layered dynamic regulation for improving metabolic pathway productivity in *Escherichia coli*. *Proc Natl Acad Sci USA* 115(12):2964–2969
- Fuqua WC, Winans SC, Greenberg EP (1994) Quorum sensing in bacteria: the LuxR-LuxI family of cell density-responsive transcriptional regulators. *J Bacteriol* 176(2):269–275
- Ge C, Sheng HK, Chen X, Shen XL, Sun XX, Yan YJ, Jia W, Yuan QP (2020) Quorum sensing system used as a tool in metabolic engineering. *Biotechnol J* 15(6):1900360
- Gupta A, Reizman IMB, Reisch CR, Prather KL (2017) Dynamic regulation of metabolic flux in engineered bacteria using a pathway-independent quorum-sensing circuit. *Nat Biotechnol* 35(3):273–279
- Harder BJ, Bettenbrock K, Klamt S (2018) Temperature-dependent dynamic control of the TCA cycle increases volumetric productivity of itaconic acid production by *Escherichia coli*. *Biotechnol Bioeng* 115(1):156–164
- Høyland-Kroghsbo NM, Paczkowski J, Mukherjee S, Broniewski J, Westra E, Bondy-Denomy J, Bassler BL (2017) Quorum sensing controls the *Pseudomonas aeruginosa* CRISPR-Cas adaptive immune system. *Proc Natl Acad Sci USA* 114(1):131–135
- Jiang XR, Yan X, Yu LP, Liu XY, Chen GQ (2021) Hyperproduction of 3-hydroxypropionate by *Halomonas bluephagenesis*. *Nat Commun* 12(1):1513
- Kaur G, Srivastava A, Chand S (2015) Debottlenecking product inhibition in 1,3-propanediol fermentation by *in-situ* product recovery. *Bioresour Technol* 197:451–457
- Kelly CL, Harris AWK, Steel H, Hancock EJ, Heap JT, Papachristodoulou A (2018) Synthetic negative feedback circuits using engineered small RNAs. *Nucleic Acids Res* 46(18):9875–9889
- Kim EM, Woo HM, Tian T, Yilmaz S, Javidpour P, Keasling JD, Lee TS (2017) Autonomous control of metabolic state by a quorum sensing (QS)-mediated regulator for bisabolene production in engineered *E. coli*. *Metab Eng* 44:325–336
- Lan EI, Liao JC (2012) ATP drives direct photosynthetic production of 1-butanol in cyanobacteria. *Proc Natl Acad Sci USA* 109(16):6018–6023
- Levin-Karp A, Barenholz U, Barea T, Dayagi M, Zelbuch L, Antonovsky N, Noor E, Milo R (2013) Quantifying translational coupling in *E. coli* synthetic operons using RBS modulation and fluorescent reporters. *ACS Synth Biol* 2(6):327–336
- Ling C, Qiao GQ, Shuai BW, Olavarria K, Yin J, Xiang RJ, Song KN, Shen YH, Guo Y, Chen GQ (2018) Engineering NADH/NAD⁺ ratio in *Halomonas bluephagenesis* for enhanced production of polyhydroxyalkanoates (PHA). *Metab Eng* 49:275–286
- Liu J, Li H, Xiong H, Xie X, Chen N, Zhao G, Caiyin Q, Zhu H, Qiao J (2019) Two-stage carbon distribution and cofactor generation for improving L-threonine production of *Escherichia coli*. *Biotechnol Bioeng* 116(1):110–120
- Lou W, Tan X, Song K, Zhang S, Luan G, Li C, Lu X (2018) A specific single nucleotide polymorphism in the ATP synthase gene significantly improves environmental stress tolerance of *Synechococcus elongatus* PCC 7942. *Appl Environ Microbiol* 84(18):e01222–e01218
- Mazumdar S, Clomburg JM, Gonzalez R (2010) *Escherichia coli* strains engineered for homofermentative production of D-lactic acid from glycerol. *Appl Environ Microbiol* 76(13): 4327–4336
- Moreno-Gámez S, Sorg RA, Domenech A, Kjos M, Weissing FJ, van Doorn GS, Veening J-W (2017) Quorum sensing integrates environmental cues, cell density and cell history to control bacterial competence. *Nat Commun* 8(1):1–12
- Papenfert K, Bassler BL (2016) Quorum sensing signal–response systems in Gram-negative bacteria. *Nat Rev Microbiol* 14(9):576–588
- Patterson AG, Jackson SA, Taylor C, Evans GB, Salmond GP, Przybilski R, Staals RH, Fineran PC (2016) Quorum sensing controls adaptive immunity through the regulation of multiple CRISPR-Cas systems. *Mol Cell* 64(6):1102–1108
- Peters G, De Paepe B, De Wannemaeker L, Duchi D, Maertens J, Lammertyn J, De Mey M (2018) Development of N-acetylneuraminic acid responsive biosensors based on the transcriptional regulator NanR. *Biotechnol Bioeng* 115(7):1855–1865
- Pfleger BF, Pitera DJ, Smolke CD, Keasling JD (2006) Combinatorial engineering of intergenic regions in operons tunes expression of multiple genes. *Nat Biotechnol* 24(8):1027–1032
- Salis HM, Mirsky EA, Voigt CA (2009) Automated design of synthetic ribosome binding sites to control protein expression. *Nat Biotechnol* 27(10):946–950
- Sun S, Zhang H, Lu S, Lai C, Liu H, Zhu H (2016) The metabolic flux regulation of *Klebsiella pneumoniae* based on quorum sensing system. *Sci Rep* 6(1):1–9
- Surette MG, Bassler BL (1998) Quorum sensing in *Escherichia coli* and *Salmonella typhimurium*. *Proc Natl Acad Sci USA* 95(12):7046–7050
- Takpho N, Watanabe D, Takagi H (2018) High-level production of valine by expression of the feedback inhibition-insensitive acetoacetylase synthase in *Saccharomyces cerevisiae*. *Metab Eng* 46:60–67
- Tan SZ, Prather KL (2017) Dynamic pathway regulation: recent advances and methods of construction. *Curr Opin Chem Biol* 41:28–35
- Thomas PW, Stone EM, Costello AL, Tierney DL, Fast W (2005) The quorum-quenching lactonase from *Bacillus thuringiensis* is a metalloprotein. *Biochemistry* 44(20):7559–7569
- Wang J, Zhao P, Li Y, Xu L, Tian P (2018) Engineering CRISPR interference system in *Klebsiella pneumoniae* for attenuating lactic acid synthesis. *Microb Cell Factories* 17(1):1–12
- Wang T, Wang M, Zhang Q, Cao S, Li X, Qi Z, Tan Y, You Y, Bi Y, Song Y (2019) Reversible gene expression control in *Yersinia pestis* by using an optimized CRISPR interference system. *Appl Environ Microbiol* 85(12):e00097–e00019
- Williams T, Averagesch N, Winter G, Plan M, Vickers C, Nielsen L, Krömer J (2015) Quorum-sensing linked RNA interference for dynamic metabolic pathway control in *Saccharomyces cerevisiae*. *Metab Eng* 29:124–134
- Wu J, Bao M, Duan X, Zhou P, Chen CW, Gao, JH, Cheng SY, Zhuang QQ, Zhao ZJ (2020a) Developing a pathway-independent and full-autonomous global resource allocation strategy to dynamically switching phenotypic states. *Nat Commun*, 11: 5521 | <https://doi.org/10.1038/s41467-020-19432-2>
- Wu J, Chen W, Zhang Y, Zhang X, Jin JM, Tang SY (2020b) Metabolic engineering for improved curcumin biosynthesis in *Escherichia coli*. *J Agric Food Chem* 68(39):10772–10779
- Xu P, Li L, Zhang F, Stephanopoulos G, Koffas M (2014) Improving fatty acids production by engineering dynamic pathway regulation and metabolic control. *Proc Natl Acad Sci USA* 111(31):11299–11304
- Xu X, Williams TC, Divne C, Pretorius IS, Paulsen IT (2019) Evolutionary engineering in *Saccharomyces cerevisiae* reveals a TRK1-dependent potassium influx mechanism for propionic acid tolerance. *Biotechnol Biofuels* 12(1):1–14
- You L, Cox RS, Weiss R, Arnold FH (2004) Programmed population control by cell–cell communication and regulated killing. *Nature* 428(6985):868–871
- Zhou S, Grabar TB, Shanmugam KT, Ingram LO (2006a) Betaine tripled the volumetric productivity of D (-)-lactate by *Escherichia coli* strain SZ132 in mineral salts medium. *Biotechnol Lett* 28(9):671–676
- Zhou S, Shanmugam KT, Yomano LP, Grabar TB, Ingram LO (2006b) Fermentation of 12% (w/v) glucose to 1.2 M lactate by *Escherichia coli* strain SZ194 using mineral salts medium. *Biotechnol Lett* 28(9):663–670
- Zhou L, Niu DD, Tian KM, Chen XZ, Prior BA, Shen W, Shi GY, Singh S, Wang ZX (2012) Genetically switched D-lactate production in *Escherichia coli*. *Metab Eng* 14(5):560–568

Publisher's Note

Springer Nature remains neutral with regard to jurisdictional claims in published maps and institutional affiliations.